Insight into the storage-related oxidative/hydrolytic degradation of olive oil secoiridoids by liquid-chromatography and high-resolution Fourier-transform mass spectrometry

R. Abbattista[a], I. Losito[a,b *], A. Castellaneta[a], C. De Ceglie[a, **], C.D. Calvano[b,c], T.R.I. Cataldi[a,b]

[a]*Dipartimento di Chimica, Università degli Studi di Bari "Aldo Moro", via Orabona 4, 70126 Bari (Italy)*

[b]*Centro Interdipartimentale SMART, Università degli Studi di Bari "Aldo Moro", via Orabona 4, 70126 Bari (Italy)*

[c]*Dipartimento di Farmacia e Scienze del Farmaco, Università degli Studi di Bari "Aldo Moro", via Orabona 4, 70126 Bari (Italy)*

Number of Figures: 7
Supporting Information: Yes

Running title: Degradation of secoiridoids during EVOO storage

*Corresponding Author, e-mail: ilario.losito@uniba.it, phone: 0039 080 5442506

**Current address: *Istituto di Ricerca sulle Acque - Consiglio Nazionale delle Ricerche (IRSA-CNR), Viale Francesco de Blasio, 5, 70132 Bari (Italy)*

Abstract

The study of negative effects potentially exerted by the exposure to oxygen and/or light, and thus also by the type of container, on the quality of extra-virgin olive oil (EVOO) during its prolonged storage requires an appropriate choice of analytical methods and of components to be monitored. Here, reverse phase liquid chromatography coupled to high resolution/accuracy Fourier-transform mass spectrometry with Electrospray Ionization (RPLC-ESI-FTMS) was exploited to study oxidative/hydrolytic degradation processes occurring on the important bioactive components of EVOO known as secoiridoids, *i.e.*, oleuropein and ligstroside aglycones, oleacin and oleocanthal, during storage up to 6 months under controlled conditions. Specifically, isomeric oxidative by-products resulting from the transformation of a carbonylic group of the original secoiridoids into a carboxylic one, and compounds resulting from hydrolysis of the ester linkage of secoiridoids, *i.e.*, elenolic and decarboxymethyl-elenolic acids and tyrosol and 3-hydroxytyrosol, were monitored, along with their precursors. Data obtained from EVOO storage at room temperature in glass bottles with/without exposure to light and/or oxygen indicated that, although it was more relevant if a periodical exposure to oxygen was performed, a non negligible oxidative degradation occurred on secoiridoids also when nitrogen was used to saturate the container headspace. In a parallel experiment, the effects of storage of the same EVOO (250 mL) for up to six months in containers manufactured with different materials/shapes were considered. In particular, a square dark glass bottle, a stainless steel can and a ceramics jar, typically used for EVOO commercialization, and a clear polyethylene terephthalate (PET) bottle, purposely chosen to prompt secoiridoid degradation through exposure to light and to oxygen, were compared. Dark glass was found to provide the best combined protection of major secoiridoids from oxidative and hydrolytic degradation, yet the lowest levels of oxidized by-

products were observed when the stainless-steel can was used.

Keywords: secoiridoids, extra-virgin olive oil, oxidative/hydrolytic degradation, olive oil storage, high resolution mass spectrometry

Introduction

Secoiridoids are natural organic compounds synthesized by several plants, including those of the *Oleaceae* family, like olive (*Olea europea L.*), and represent one of the most interesting components among phenolics included in the non-saponifiable fraction of extra-virgin olive oil (EVOO)[1]. Their nutraceutical benefits and the role played in influencing the product quality and sensory attributes have been the object of several studies over the last two decades[1-9]. Major secoiridoids detected in olive oil arise from precursors contained in olive drupes (and leaves, if included in the first stage of oil production), *i.e.*, oleuropein and ligstroside, corresponding to esters formed, respectively, by tyrosol (*p*-hydroxy-phenylethyl alcohol, HPEA) or 3-hydroxy-tyrosol (3,4-dihydroxy-phenylethyl alcohol, 3,4-DHPEA) and the glycosidic derivative of a carboxylic acid known as elenolic acid (IUPAC name 2-[(2S,3S,4S)-3-formyl-5-methoxycarbonyl-2-methyl-3,4-dihydro-2H-pyran-4-yl]acetic acid, usually abbreviated as EA), which is the actual secoiridoid. The interplay between enzymatic and chemical reactions occurring at different stages of olive oil production leads to the generation of four major compounds, namely oleuropein and ligstroside aglycones, often abbreviated as 3,4-DHPEA-EA and HPEA-EA, respectively, and oleac(e)in and oleocanthal, with both the latter including a decarboxymethylated form of elenolic acid (often referred to as EDA), thus usually abbreviated as 3,4-DHPEA-EDA and HPEA-EDA, respectively (see Ref. 1 and references cited therein).

Research work performed over more than three decades, based initially on UV and NMR spectroscopies and then also on mass spectrometry (MS), has unveiled many structural details of the four compounds, emphasizing the presence of several isomers for most of them[10-23]. Recently, a systematic investigation performed in our laboratory, based on reverse phase liquid chromatography coupled to high resolution/accuracy Fourier-transform single and tandem mass

spectrometry with electrospray ionization (RPLC-ESI-FTMS and MS/MS), integrated by H/D exchange, has elucidated the identity of those isomeric forms in the case of oleuropein and ligstroside aglycones[24-25]. Using the same approach, the presence of isomers, although in a lower number, has also been demonstrated for oleocanthal and oleacin[26]. In **Figure 1** a summary is reported for all the isomeric forms identified for the four compounds in olive oil, labelled as *Open Forms I* and *II* and *Closed Forms I* and *II*, depending on the specific structure assumed by the elenolic or decarboxymethyl-elenolic acid moiety included in their molecules, like in our recent papers[24-25]. The structural variability emphasized in the figure arises from the reactivity of a hemiacetal moiety originated from the β-glucosidase catalyzed detachment of the glucose unity initially present in oleuropein and ligstroside. Cyclizations to form dihydropyranic rings, through an intra-molecular 1,4-Michael addition, are included among possible reactions[24-25]. The remarkable number of isomeric forms found for secoiridoids in olive oil is due to the contemporary occurrence of diastereoisomerism (see stereogenic centers labelled with an asterisk in **Figure 1**, including the original chiral centre on C^5) and positional/geometric isomerism (see the geometry of the C^8=C^9 double bond in *Open Forms I* and the alternative location of the C=C bond between C^8 and C^{10} in *Open Forms II*). As emphasized by H/D exchange experiments performed during our previous studies[24-25], this scenario is made even more intricate by the presence of stable enolic counterparts of aldehydic groups, whose structures were not depicted in **Figure 1**.

The reactivity of aldehydic moieties (one or two) present in all isomeric secoiridoids represents a matter of concern when prolonged storage of EVOO takes place, since it may lead to their transformation into by-products with a potentially lower bioactivity, and eventually able to alter the organoleptic features of the product. For this reason, the evolution during olive oil

storage of secoiridoids, among phenolic compounds, has been studied since the late 1990s[27]. Acid-catalyzed hydrolytic processes, leading to the release of tyrosol/3-hydroxytyrosol and of elenolic acid or its decarboxymethylated counterpart were soon evidenced in the case of secoiridoids[28]. In subsequent years, the oxidation of a secoiridoid aldehydic moiety to carboxylic acid was invoked[29]. This process can be considered an alternative oxidative pathway with respect to the well known oxidation of the catecholic moiety of oleuropein aglycone and oleacin to *o*-benzoquinone, which occurs also on free 3-hydroxytyrosol contained in EVOO, making these compounds interesting scavengers of Reactive Oxygen Species (ROS), like singlet-state oxygen (*vide infra*), and of peroxy-alkyl readicals (ROO•) generated by lipid autoxidation during EVOO storage (see Ref. 7 and references cited therein). The decrease in the amount of secoiridoids upon prolonged storage (up to 22 months) of olive oil, resulting also from the described degradative phenomena, has been systematically confirmed by several investigations over the last decade[30-35]. Many of these studies confirmed the presence of oxidized derivatives of major secoiridoids with a nominal molecular mass shift of 16 Da, thus implying the introduction of an oxygen atom on their structures. The interpretation of this process as the transformation of a C=O group into a COOH one was emphasized in papers based on mass spectrometry, sometimes integrated by NMR spectroscopy, both for the aglycones of oleuropein and ligstroside[18] and for oleacin and oleocanthal, whose carboxylic derivatives have been recently defined *oleaceinic* and *oleocanthalic* acids[36,37]. Singlet state oxygen, whose generation is involved in olive oil photoxidation[38], might play a relevant role also in the oxidation of aldehydic groups of secoiridoids to carboxylic ones[39]. As for other EVOO components, the integrity of secoiridoids should thus benefit from the minimization of olive oil exposure to oxygen and, at the same time, to light, since the latter can enhance the generation of ROS through the intervention of EVOO

components acting as photosensitizers[38]. For this reason, the protection from light is usually considered a key factor to preserve olive oil quality during prolonged storage at room temperature (see, for example, Ref. 40).

Starting from these considerations, a series of parallel storage experiments, lasting up to 6 months, was set up in our laboratory for a specific EVOO, locally produced (*Apulia* region, Southern Italy) from the *Coratina* cultivar. In particular, the evolution of oxidized (specifically, carboxylic acids) and hydrolytic derivatives of major secoiridoids was investigated using the same analytical approach recently adopted in our laboratory to characterize unmodified EVOO secoiridoids, based on RPLC-ESI-FTMS[24-26]. The effect of exposure to light and/or to oxygen at room temperature for aliquots of the olive oil stored in a glass bottle typically used for commercialization was assessed as a part of the experiment. The influence of four different storage containers, three of which commonly used for commercial purposes, i.e. a square dark glass bottle, a ceramics jar, a stainless steel can, and a clear polyethyleneterephtalate bottle, on the oxidation/hydrolysis of secoiridoids upon prolonged storage was also evaluated under real-life conditions. Indeed, a periodical exposure of the olive oil to atmospheric oxygen, mimicking that occurring in a domestic context, where small aliquots are periodically withdrawn from the container, for cooking/dressing purposes, was performed during the experiment.

Materials and methods

Chemicals and olive oil sample

The following chemicals: water, methanol and acetonitrile (LC-MS grade), n-hexane (HPLC-grade), and oleuropein (2-(3,4-dihydroxyphenyl)ethyl-(2S-(2α,3E,4β))-3-ethylidene-2-(β-D-glucopyranosyloxy) - 3,4-dihydro-5-(methoxycarbonyl)-2H-pyran-4-acetate), were obtained

155 from Sigma-Aldrich (Milan, Italy). An Italian EVOO produced in the *Apulia* region of Italy during
156 the 2018/2019 campaign, using olives of cv. *Coratina,* was selected for the present study. In the
157 specific case, a blade crusher was adopted for olive crushing, then malaxation of the olive paste
158 was performed at 26°C for 25 min, followed by horizontal centrifugation in a three-phase
159 decanter. The final separation between water and oil was achieved by natural decantation,
160 instead of vertical centrifugation, then the oil was filtered using a filter press equipped with
161 cellulose paper filters and finally stored inside a stainless steel silo whose headspace was
162 saturated with nitrogen to minimize oxidative deterioration. To keep as low as possible the
163 incidence of degradative phenomena before starting with the experiments, the EVOO amount
164 required for storage experiments (about 4 L) was sampled from the industrial silo just two days
165 after production. In the same day of withdrawal, the phenolic extracts required for preliminary
166 RPLC-ESI-FTMS analysis of secoiridoids (time 0) were prepared, then parallel storage experiments
167 were started.
168
169 **Extraction of secoiridoids from extra-virgin olive oils**
170 As mentioned in the previous section, the first extraction of secoiridoids from the selected
171 EVOO was performed at its arrival in the laboratory, using a CH_3OH/H_2O 60:40 (v/v) mixture,
172 according to the protocol succesfully adopted in our laboratory for the extraction of olive oil
173 secoiridoids[24-26], in turn adapted from those reported previously by Vichi *et al*. [18] and Ricciutelli
174 *et al*.[41]. Specifically, 2 g of extra virgin olive oil were dissolved into 3 mL of HPLC-grade hexane
175 and vortexed for 1 min; 500 μL of the extracting solvent mixture were subsequently added. The
176 resulting mixture was vortexed for 2 min and then sonicated for 4 min using a DU-32 ultrasonic
177 bath (Argo Lab, Carpi, Italy), operated at 40 kHz frequency, 120 W power and 23°C temperature.

178 The separation of the hexane-rich phase from the methanolic-aqueous one was accomplished by
179 centrifugation at 2000 g for 5 minutes. The methanolic-aqueous phase, including secoiridoids,
180 was carefully withdrawn with a microsyringe and stored in a glass tube with headspace saturated
181 with nitrogen, whereas the hexane-rich phase was subjected to a further extraction with 500 μL
182 of the extracting solvent mixture, aiming at removing eventual residual secoiridoids. The two
183 aliquots of metanolic-aqueous extract were finally pooled, washed for 1 min with 2 mL of n-
184 hexane under vortexation, to remove eventual residual apolar compounds, and then centrifuged
185 for 5 min at 2000 g, to separate the methanolic-aqueous phase. The latter was subsequently
186 stored at +4°C in a glass vial, closed with a screw cap, whose headspace was saturated with
187 nitrogen to minimize the eventual oxidation of extracted secoiridoids before RPLC-ESI-FTMS
188 analysis. To obtain a combined estimate of extraction and LC-MS analysis reproducibility, two 2
189 g aliquots of each EVOO sample considered in the present study were subjected to extraction for
190 each of the considered samples.

191 It is worth noting that, as emphasized in our recent paper[26], the relatively short time interval
192 in which secoiridoids were exposed to methanol at room temperature during the extraction
193 procedure, and then the storage of the methanol-containing extract at low temperature (+4°C)
194 before analysis, minimized their transformation into methanol-involving hemiacetals/acetals,
195 whose incidence, with respect to the precursors, never exceeded 5% (estimated from the
196 respective normalized MS responses, *vide infra*). Moreover, the incidence of further artificial
197 derivatives potentially generated during the extraction in an aqueous-methanolic mixture, *i.e.*,
198 secoiridoids hydrated on their aldehydic moiety/moieties, was found to be even more limited,
199 likely due to the lower stability of those compounds.
200

Prolonged storage of olive oil with/without exposure to light and/or to atmospheric oxygen

To compare the effect of exposure to light and/or atmospheric oxygen on secoiridoids (Experiment A) four 250 mL aliquots of the selected EVOO were transferred into as many glass bottles with square section and screw cap, like those typically used for the commercialization of 250 mL of olive oil, kindly donated by a local producer. Two of those bottles were fabricated using clear glass, the other two with dark glass, the latter being the most frequently (although not exclusively) adopted for olive oil commercialization, due to its light-shielding capabilities. As an example, one of the dark glass bottles adopted is shown in **Figure S1** of the Supporting Information. In a preliminary stage of the experiment, one of the bottles was filled with oil and then the volume of the latter was measured through transfer into a graduated cylinder. The difference between this volume and 250 mL, ca. 25 mL, was thus considered an estimate of the headspace available in each of the four bottles during storage. As described in the schematic experimental plan reported in **Figure S2** of the Supporting Information, the headspaces of one clear glass and one dark glass bottle were saturated with nitrogen soon after transferring the olive oil. The bottles were then ermetically closed and subsequently opened only after 1, 2, 3 and 6 months of storage, to enable the rapid withdrawal of two 2 g aliquots to be used for secoiridoids extraction and subsequent LC-MS analysis. The withdrawal was performed after a rapid (30 s) but gentle agitation of each bottle, to homogenize eventual differences in concentration of oxidized/hydrolytic by-products occurring between the headspace/oil interface and the oil bulk. It is worth noting that a preliminary test, based on a clear PET bottle filled with 250 mL of the selected EVOO and stored in natural (not direct) light for 2 months, *i.e.*, under conditions enhancing the oxidative degradation of secoiridoids (*vide infra*), was performed to assess the eventual occurrence of concentration disomogenities of by-products with respect to the

sampling depth. Specifically, 2 g aliquots of the stored oil were subsequently withdrawn, using a glass syringe with a long needle, one just below the headspace/oil interface and the other close to the bottle bottom. Upon extraction and RPLC-ESI-FTMS analysis, the differences in normalized responses obtained for oxidized derivatives of secoiridoids were within the typical variations observed for replicated extraction/analyses (*vide infra*). Among hydrolytic by-products, 3-hydroxytyrosol and elenolic acid exhibited a more relevant increase in concentration near the headspace/oil interface, compared to bulk, with differences of +34% and +14% respectively.

After each withdrawal, the headspace of each bottle was carefully filled again with nitrogen and the bottle was closed. The described experiment aimed at evaluating the effect of exposure to light when oxygen availability in the container was potentially minimized, thus the bottles were stored on a laboratory bench, where natural, but not direct, light was available for a time ranging from 8 to 14 hours a day, according to the month. The other two glass bottles selected for Experiment A (one manufactured with clear glass, the other with dark glass, see the left side of the Experiment A scheme in **Figure S2**) were kept in the same place but used for a different type of storage, *i.e.*, to simulate the periodical opening of the container occurring in a domestic environment (*e.g.*, to withdraw aliquots for cooking/dressing purposes) and, at the same time, considering also the effect of exposure to natural light for EVOO stored in a clear glass bottle. Indeed, after the initial transfer of olive oil (time 0), the bottles were closed with their caps but then they were systematically opened to air for five minutes every three days. Like for the first part of Experiment A, two 2 g aliquots were withdrawn (after a preliminary gentle agitation) from each bottle after 1, 2, 3 and 6 months and subjected to secoiridoids extraction and LC-MS analysis of the resulting extracts. All the described experiments were performed at laboratory temperature (23 ± 2 °C).

Prolonged storage of olive oil in containers fabricated with different materials and periodically exposed to atmospheric oxygen

Four containers were selected to study the effect of the container material/shape on the long-term stability of EVOO secoiridoids under domestic-like conditions, *i.e.*, upon periodic opening (5 minutes every three days) to the atmosphere (see the scheme of Experiment B in **Figure S2**). Three of the four containers, kindly donated by an EVOO local producer, were similar to those commonly used for the commercialization of 250 mL of olive oil, thus enabling a reproduction of real-life conditions. As shown in **Figure S1** of the Supporting Information, those containers were: 1) a square section dark glass bottle with screw cap (the same adopted for one of the sections of Experiment A); 2) a stainless steel can with a long neck equipped with a special anti-refill tip and a screw cap; 3) a ceramics jar with trunk conical bottom and a pressure cap, representing an old-fashioned container for olive oil, usually adopted in Southern Italy for the product commercialization as a gift (the jars are often decorated artistically at this aim). In addition, a PET bottle (total capacity 330 mL) was selected as a container potentially boosting olive oil degradation, due to exposure to light and to a non negligible continuous permeation of oxygen through the bottle wall, in addition to oxygen entering periodically during opening stages.

The containers were first rinsed internally with a small amount of the selected olive oil, then the estimates of the respective headspaces were performed as described before for the glass bottles. Due to the different shape and capacity of each container, and the equality of the transferred olive oil volume, the resulting headspace volumes were not the same, yet, since this is the actual condition for the commercialization of 250 mL volumes of the product in different types of containers, this variability was purposely not compensated. Nonetheless, the eventual

269 influence of the HS differences on the outcome of storage experiments was considered when
270 comparing the results obtained for each container (*vide infra*).

271 Like in one of the sections of Experiment A, the four containers were systematically opened
272 to the atmosphere for five minutes every three days and then two 2 g aliquots of oil were
273 withdrawn from each of them after 1, 2, 3 and 6 months since the beginning of the experiment.
274 All the described experiments were performed at room temperature (23 $\pm$ 2 °C), with containers
275 placed on the same bench adopted for Experiment A, thus under the same light exposure
276 conditions.

277

278 **RPLC-ESI-FTMS instrumentation and operating conditions**

279 An Ultimate 3000 UHPLC system coupled to a Q-Exactive quadrupole-Orbitrap mass
280 spectrometer (Thermo Scientific, Waltham, MA, USA) was used for RPLC-ESI-FTMS analyses of
281 extracts obtained from EVOO aliquots withdrawn during storage experiments. LC separations
282 were performed using an Ascentis Xpress C18 column (150 x 2.1 mm ID, 2.7 μm particle size)
283 preceded by an Ascentis Xpress C18 (5 x 2.1 mm ID) security guard cartridge (Supelco). 5 μL of
284 olive oil extracts, previously spiked with oleuropein 100 mg/L, used as internal standard (*vide*
285 *infra*), and then diluted 1:10 (v/v) with the extraction solvent mixture, were injected in the C18
286 column using the autosampler included in the Ultimate 3000 UHPLC system, equipped with a 6-
287 way Rheodyne valve.

288 Separations were performed using the following elution gradient, based on water (solvent
289 A) and acetonitrile (solvent B), already adopted in our laboratory for the separation of isomeric
290 secoiridoids in olive oil extracts[24-26]: 0 - 5 min) 20% solvent B; 5 - 35 min) from 20% to 50% (v/v)
291 solvent B; 35-40 min) from 50% to 100% of solvent B; 40 – 50 min) isocratic at 100% solvent B;

50 – 55 min) from 100% to 20% of solvent B; 55 – 70 min) column reconditioning at 20 % solvent B. The flow rate was always set at 200 µL/min and the column temperature at 25 °C. All major secoiridoids and their eventual oxidative by-products could be easily detected as $[M-H]^-$ ions, as a result of deprotonation occurring during the ESI process, involving a phenolic OH group or a COOH group, according to the case, thus negative polarity was always adopted for MS detection.

Specifically, ESI(-)-FTMS *full scan* acquisitions were performed in the *m/z* range 100 – 1500 after setting the main parameters of the heated ESI (HESI) interface and of the ion optics of the Q-Exactive spectrometer as follows: sheath gas flow rate, 60 (arbitrary units); auxiliary gas flow rate, 15 (arbitrary units); spray voltage, -4 kV; capillary temperature, 200 °C; S-lens RF level, 100 (arbitrary units). High resolution MS/MS analyses were performed by isolating only the first isotopologue of the $[M-H]^-$ ion of each secoiridoid of interest (1 *m/z* unit-wide isolation window) in the quadrupole analyzer of the Q-Exactive spectrometer and fragmenting it into the Higher energy Collisional Dissociation (HCD) cell, after setting the Normalized Collisional Energy (NCE) as 20 (a.u.). Both MS and MS/MS acquisitions were performed by setting the resolving power of the Q-Exactive spectrometer at its maximum (120000 at *m/z* 200). This resulted in a resolving power always better than 110000 for signals related to all analytes (note that the resolvng power of an Orbitrap mass analyzer decreases at the increase of the *m/z* ratio). The spectrometer was calibrated daily, before starting LC-MS analyses, through infusion-ESI(-)-FTMS analysis of the Pierce™ Negative Ion Calibration Solution (sodium dodecyl sulfate 2.9 µg/mL, sodium taurocholate 5.4 µg/mL and 0.001% Ultramark 1621), as recommended by the spectrometer manufacturer. As a result, a mass accuracy always better than 2 ppm was achieved on *m/z* ratios related to the analytes.

The LC-MS instrumentation was controlled by the Xcalibur software (Thermo Scientific),

used also for ion current extraction. The ChemDraw Pro 8.0.3 software (CambridgeSoft Co., Cambridge, MA, USA) was employed to draw chemical structures and evaluate possible fragmentation pathways. The Microcal Origin® 6.0 software (Microcal Software Inc., Northampton, MA, USA) was used to obtain plots of secoiridoid responses vs storage time.

Results and discussion

Recognition of major secoiridoids and of their oxidative/hydrolytic by-products in extracts of stored EVOO samples by RPLC-ESI-FTMS

As mentioned before, the EVOO selected for the present study was subjected to extraction in duplicate of secoiridoids and other polar compounds, followed by extract analysis by RPLC-ESI(-)-FTMS analysis, just at the arrival into the laboratory, two days after production (time 0). The eXtracted Ion Current (XIC) chromatograms obtained for the four major secoiridoids of olive oil from one of the replicated extracts are displayed in **Figure 2**. Ion current extraction windows centered on the exact *m/z* ratios of the first isotopologues of their $[M-H]^-$ ions and having a 0.004 *m/z* units width were adopted, to minimize any eventual interference due to quasi-isobaric compounds. Since a maximum shift of $\pm$0.0006 units was observed between experimental and theoretical *m/z* ratios, such intervals were able to provide a correct extraction of ion currents.

As previously demonstrated by us[24-26] and by other Authors using LC-MS[15,18], a complex combination of peaks referred to isomeric species was found for the aglycones of oleuropein (OA) and ligstroside (LA). In the present case peaks detected in the respective XIC traces were labelled in accordance with the numeration adopted in our previous papers[24-26] and used also in **Figure 1**, thus the following elution order (increasing retention time) was observed: *Open Forms I – Open Forms II - Closed Forms I – Closed Forms II*, with *Open Forms I* prevailing in terms of

response for both secoiridoids in this specific case. In agreement with our previous results[24-26], XIC traces obtained for oleacin and oleocanthal were significantly simpler, due to the more limited structural variability of these secoiridoids. This feature is related to the absence of the carboxymethylic ($-CO_2CH_3$) moiety on C^4 in their molecular structure (see **Figure 1**), with consequent lack of a stereogenic center on that carbon atom, in turn reducing the number of potential diastereoisomers for open forms, compared to OA and LA. Moreover, the lack of the CO_2CH_3 moiety prevents *Closed Forms II* (originating from an intramolecular 1,4-Michael addition after its enolization[24,25]) from being formed. As a result, the chromatographic profiles of oleocanthal and oleacin were dominated by just two almost identical peaks. Interestingly, ions with a *m/z* ratio consistent with the theoretical values 249.0769, for oleacin, and 233.0819, for oleocanthal, were detected in MS/MS spectra averaged under both peaks. As emphasized in the top panel of **Figure S3** in the Supporting Information, these values could be interpreted with a specific fragmentation, namely, the neutral loss of 3-butenone, occurring upon breakage of the C^5-C^9 bond, with a concurrent 1,3 H transfer towards C^9. This process is plausible only for *Open Forms II* of oleacin and oleocanthal, being their C^9 atom not involved in a C=C bond. Moreover, since C^9 is a stereogenic center only in *Open Forms II*, the two prevailing peaks observed in the XIC traces of oleacin and oleocanthal appear to be referred to diasteroisomers arising from the two possible couplings between the fixed configuration at C^5 (the original chiral center) and the two possible configurations at C^9 (see **Figure 1**).

The latest eluting peak in the case of oleocanthal (r.t. 22.11 min, see **Figure 2**) was tentatively related to one of its possible *Closed Forms I* (four diastereoisomers, at least in principle, see **Figure 1**) in our recent study[26]. This hypothesis was confirmed in the present work by the detection of a peculiar couple of product ions in the corresponding MS/MS spectrum, compatible

with exact *m/z* ratios 137.0244 and 137.0608. As shown in the bottom panel of **Figure S3**, these ions arise from a series of fragmentations starting from a further product ion detected in the MS/MS spectrum of oleocanthal (the enolate of decarboxymethyl-elenolic acid, exact *m/z* 183.0663) and possible only for *Closed Forms I* of oleocanthal.

It is worth noting that, differently from oleocanthal, the two lately eluting peaks detected in the XIC trace of oleacin (r.t. 15.85 and 16.81 min, see **Figure 2**) were not related to closed forms of this secoiridoid but to the carboxylic acid of oleocanthal (*alias* oleocanthalic acid), which has the same molecular formula of oleacin. Peaks related to oleocanthalic acid could be easily recognized using MS/MS analysis, since a peculiar fragment with *m/z* ratio compatible with the exact value 199.0612, corresponding to the first isotopologue of the $[M-H]^-$ ion of decarboxymethyl-elenolic acid (in open or closed form) having an aldehydic C=O group turned into a COOH one was observed in the corresponding MS/MS spectra (*vide infra*), in accordance with our previous work[26]. **Figure 2** is completed by the chromatographic profile obtained for oleuropein, which was preliminarily added as an internal standard (100 mg/L concentration) to all the analyzed olive oil extracts. The XIC peak area of oleuropein was used to normalize those related to all the secoiridoids of interest and to their oxidative/hydrolytic by-products. This normalization was mandatory to make a reliable quantitative comparison between samples analyzed after the long time intervals required by storage experiments (up to 6 months), considering that fluctuations in the absolute instrumental response may occur on a much shorter time range in the case of ESI-MS. Notably, oleuropein could be used as internal standard (IS) since the preliminary analysis of a not spiked aliquot of the selected EVOO extract showed that it was totally absent, as expected. Additionally, oleuropein shares a relevant part of its molecular

structure with most analytes of interest in this study, and even its most likely ionization site, i.e., one of the phenolic OH groups, with the four major secoiridoids monitored.

XIC traces like those reported in **Figure 2** were systematically obtained for all the samples analyzed during the present study. For the sake of comparison, those obtained for the four major secoiridoids and for oleuropein IS from the olive oil stored for 6 months in a dark glass bottle under domestic-like conditions (i.e., periodic exposure to atmospheric oxygen) are reported in **Figure 3**. The main effect of storage on OA was a decrease on the left side of the peculiar band (#11) resulting from the partial co-elution of its isomeric *Closed Forms I*[24], with a concurrent increase in the incidence of open forms, especially *Open Forms I* labelled as 2a/2b. This evolution resembles that observed after deliberate exposure to an acidic environment of oleuropein aglycone resulting from the β-glucosidase-catalyzed artificial hydrolysis of the glycosidic bond of oleuropein[24]. The process was thus interpreted as the acid-catalyzed opening of the dihydropyranic ring of *Closed Forms I* (or *II*) of OA, with generation of the corresponding open forms. Despite the described modification and an expected decrease in the MS response of OA isomeric forms (see the normalization levels, NL, reported in **Figures 2** and **3** for the OA XIC traces and compare them to the NL levels of oleuropein in the two figures), the OA profile was qualitatively similar to that observed at time 0. The same outcome was generally observed also after prolonged storage under other conditions experimented during this study and the effect was even more evident for LA and for oleocanthal. Conversely, a new band (r.t. 12.76), appearing as the overlap of at least two close chromatographic peaks, was clearly detected in the XIC trace referred to the *m/z* ratio of the $[M-H]^-$ ion of oleacin (see **Figure 3**) and a similar feature was found also after prolonged storage under other tested conditions, with a general increase observed with storage time. The detection of the already described product ion at *m/z* 199.0612

406 in the MS/MS spectrum averaged under the 12.76 min band confirmed that it was not related to
407 a newly appearing isomer of oleacin, but to additional isomers of oleocanthalic acid.

408 As evidenced in **Figures S4** and **S5** of the Supporting Information, specific product ions
409 detected in the respective MS/MS spectra enabled a more detailed characterization of the cited
410 oleocanthalic acid isoforms. In particular, the presence of fragments with *m/z* ratios 137.0244
411 and 137.0608, already cited for oleocanthal but generated through a slightly different pathway
412 in the case of its oxidized counterpart (see **Figure S4**), indicated that peaks eluted at r.t.
413 15.82/15.85 and 16.79/16.81 min corresponded to the carboxylic derivatives of oleocanthal
414 *Closed Forms I*. On the other hand, the detection of two product ions consistent with exact ratios
415 111.0088 and 111.0815 in the corresponding MS/MS spectrum indicated the major band at r.t.
416 12.76 min to be related to oxidized derivatives of *Open Forms II* of oleocanthal (see **Figure S5**).
417 As emphasized in **Figure S5**, the generation of those product ions was compatible with both the
418 possible locations of the newly formed COOH group (*i.e.*, C^1 and C^3 atoms).

419 As a subsequent data processing, carboxylic derivatives related to OA, LA and oleacin could
420 be searched for in all the analyzed samples by extracting ion currents referred to the exact *m/z*
421 ratios of the first isotopologues of their $[M-H]^-$ ions, *i.e.*, 393.1191, 377.1242 and 335.1136,
422 respectively. As apparent, the *m/z* ratio for the carboxylic derivative of LA was identical to that
423 of OA, being the molecular formulas of their ions identical ($[C_{19}H_{21}O_8]^-$). Therefore, a careful
424 evaluation of MS/MS spectra referred to all precursor ions with *m/z* 377.1242, *i.e.*, those
425 averaged under each of the chromatographic peaks/bands detected in the OA-related XIC traces,
426 was required for all samples. Specifically, a search was made for the diagnostic product ion with
427 *m/z* ratio compatible with exact value 257.0666, corresponding to the $[M-H]^-$ ion of elenolic acid
428 with a C=O group turned into a COOH one (see **Figure S6** in the Supporting Information).

Surprisingly, no evidence was ever obtained for the presence of this fragment in MS/MS spectra referred to the *m/z* 377.1242 ion, including EVOO samples stored for up to 6 months with periodic exposure to oxygen. This result provided a further confirmation of the outcome already observed in our laboratory, on a shorter time range, for EVOOs analyzed a few days after production, i.e., the apparent absence of oxidative reactivity on the secoiridoid portion of the molecular structure of ligstroside aglycone[26]. It is worth noting that evidences for the generation of the carboxylic derivative of LA were found in our laboratory only after a one year storage in a dark glass bottle with air-filled headspace, during an experiment performed on another Apulian EVOO but still produced with *Coratina* olives. Nonetheless, the response observed for the oxidized form of LA in that oil was the lowest among those found for oxidative by-products of major secoiridoids (data not shown). These results agree with those reported by Carrasco-Pancorbo *et al.* after studying the accelerated oxidative deterioration of olive oil during severe thermal treatment (180 °C). Indeed, the Authors showed that, although its concentration (when assessed using HPLC-UV) decreased, LA resisted better than OA to thermally induced oxidative degradation on a 3 h time range and this behaviour was related to the higher oxidative stability of tyrosol derivatives, like LA, compared to 3-hydroxytyrosol ones[42].

A quite different outcome was observed for the carboxylic derivatives of OA and oleacin, as evidenced by the corresponding XIC traces reported in **Figure 3**, also referred to the extract of EVOO stored for 6 months in a dark glass bottle with periodical exposure to atmospheric oxygen. Indeed, several chromatographic peaks were detected in both cases, their number being clearly higher in the case of the OA derivative. Diagnostic product ions, *i.e.*, those confirming the transformation of a C=O group into a COOH one, compatible with exact *m/z* ratios 257.0666 and 199.0612 (see the relevant structures in **Figure S6** and **S5**, respectively), were found

452 systematically in MS/MS spectra related to precursor ions corresponding to the carboxylic
453 derivatives of OA and oleacin. Interestingly, a peculiar further product ion, compatible with an
454 exact *m/z* 101.0244, was detected for carboxylic derivatives of OA eluting after 20 min, whose
455 peaks were grouped under the common label CF in **Figure 4**. Indeed, as shown in the upper-right
456 side of **Figure S6**, the generation of this ion can be explained by isomeric structures of *Closed*
457 *Forms I* and *II* of OA in which either the C^1=O or the C^3=O group has been turned into a COOH
458 group. According to the case, the ion corresponds to the deprotonated form of 3-hydroxy-but-2-
459 enoic acid or 3-methoxy-prop-2-enoic acid (see **Figure S6**). The involvement also of closed forms
460 of OA in the carbonyl-to-carboxyl oxidation process, joined to the presence of two alternative
461 oxidation sites (C^1 or C^3) in the case of open forms of OA (see structures in **Figure S6**) and to the
462 sources of isomerism inherent to OA, explains the remarkable number of peaks detected for the
463 carboxylic derivative of this secoiridoid. Like for unmodified OA, closed forms of its carboxylic
464 derivative were eluted later than open forms, due to the enhanced hydrophobicity of the
465 dihydropyranic ring included in closed forms molecular structure.

466 As for the oxidized derivatives of oleacin, it is worth noting that peculiar product ions with
467 *m/z* 111.0088 and 111.0815, already discussed for oxidized *Open Forms II* of oleocanthal, were
468 systematically detected in MS/MS spectra of peaks eluting within 14 min in the corresponding
469 XIC trace (see **Figure 3**). Based on the same pathways shown in **Figure S5** for oxidized oleocanthal
470 (note that the starting ion in those pathways is a common fragment for the oxidized forms of
471 oleocanthal and oleacin) those peaks can be referred to *Open Forms II* of oxidized oleacin with
472 the COOH group involving either the C^1 or the C^3 atom. On the other hand, product ions with *m/z*
473 111.0088 and 111.0815 were not detected in MS/MS spectra referred to the lately eluting peaks
474 observed in the XIC trace of **Figure 3** referred to oleacin carboxylic acid (r.t. 15.05/15.87 min).

For this reason, they were tentatively assigned to closed forms of oleacin carboxylic acid; this hypothesis was also consistent with the high retention times observed for the two peaks, since closed forms of secoiridoids were always eluted late from the adopted C18 column.

Based on the results discussed so far, a relevant oxidation to carboxylic acid was found for oleocanthal but not for LA, even though both share the tyrosol structure. This evidence suggests that the better resistance of LA to oxidation to a carboxylic derivative is related to the presence of the tyrosol unit, as commented before, but also of the carboxymethyl group on C^4. A role might be played by the lower ability of LA to form chelates with metal ions contained in olive oil, which have been reported as a favoring factor for secoiridoid oxidation[43]. Indeed, LA, like oleocanthal, lacks the catechol unit on the phenolic side, that could be a possible site for chelation; moreover, the carboxymethylic moiety on C^4 might determine a steric hindrance for metal chelation by the two C=O groups of LA open forms.

In the present study, the sum of peak areas referred to all the different isomers of a specific derivative was considered as a measurement of their overall MS response and, once normalized to the XIC peak area of oleuropein, was used to monitor the incidence of those compounds as a function of storage time under different conditions (*vide infra*).

As shown in the two panels at the bottom of **Figure 3**, oxidized derivatives of elenolic acid and decarboxymethyl-elenolic acid having a COOH group instead of a C=O one could be easily monitored in all EVOO extracts by considering ions with *m/z* ratios 257.0666 and 199.0612, respectively. It is worth noting that peaks actually related to these compounds were only those eluted early from the C18 column (r.t. 1.86 and 1.62 min, respectively, in **Figure 3**), due to their more hydrophilic character. All the other peaks detected in the corresponding XIC traces, whose retention times were purposely underlined in **Figure 3** (from 4.34 to 15.87 min) were generated

498 by spontaneous fragmentation, likely occurring in the ESI source, of carboxylic derivatives of OA
499 or oleacin, according to the case, as emphasized by the excellent alignment with peaks detected
500 in the XIC traces of those compounds reported in the same figure. As a first hypothesis, the
501 presence of oxidized derivatives of elenolic and decarboxymethyl-elenolic acids could be
502 interpreted as the result of hydrolysis of the ester bond of previously oxidized OA and
503 oleacin/oleocanthal, respectively. However, the occurrence of oxidation directly on elenolic and
504 decarboxymethyl-elenolic acids previously released through ester bond hydrolysis in unmodified
505 secoiridoids could not be excluded. Indeed, elenolic and decarboxymethyl-elenolic acids were
506 clearly detected in the same EVOO extract (see **Figure S7**, Supporting Information) and in all the
507 other samples. The complex band observed in the XIC trace referred to elenolic acid emphasized,
508 once again, the inherent structural complexity of this compound, which is then transferred also
509 to structures of oleuropein and ligstroside aglycones, that include the EA one. XIC traces obtained
510 for tyrosol and 3-hydroxytyrosol, the further by-products expected from the hydrolytic
511 degradation of major EVOO secoiridoids, are also reported in **Figure S7**. To follow the extent of
512 hydrolytic degradation occurring on major secoiridoids during storage, both phenolic compounds
513 were monitored in all the examined EVOO samples (*vide infra*).

514 It is finally worth noting that a further type of oxidative by-product, specific for the two
515 secoiridoids including a catechol moiety in their structure, i.e., oleuropein aglycone and oleacin,
516 was tentatively considered during this study. Indeed, XIC traces were generated also for $[M-H]^-$
517 ions (respective exact *m/z* 375.1085 and 317.1031) of compounds resulting from the oxidation
518 of the catechol moiety to *o*-benzoquinone, which lack two hydrogen atoms with respect to their
519 precursors. Actually, peaks were found in those XIC traces, with a multiplicity reflecting that of
520 the corresponding precursors, yet the respective overall areas were much lower than those

typical of carboxylic derivatives of OA and oleacin even after six months of storage with periodical exposure to oxygen. Even considering that the ionization of *o*-benzoquinone derivatives of OA and oleacin is less efficient, under ESI conditions, than that of their precursors, due to the lack of phenolic OH groups, which are the main site of negative ionization for OA and oleacin, the observed difference suggested that the oxidation on the catechol moiety might be less relevant than that involving C=O groups. For this reason, *o*-benzoquinone derivatives were not considered further in the present investigation.

Evolution of major secoiridoids and of their oxidative/hydrolytic by-products in EVOO during prolonged storage with/without exposure to light and/or to atmospheric oxygen

Data obtained from Experiment A, *i.e.*, EVOO long term storage in dark and clear glass bottles with/without periodic exposure to atmospheric oxygen, were the first to be elaborated during this study. Indeed, they provided information on the combined effect of light and oxygen on EVOO secoiridoids, that could be useful to compare data obtained using different types of containers (Experiment B). Graphs showing the evolution, over a six months interval, of normalized XIC peak areas obtained for OA, LA, oleacin and oleocanthal in the four setups related to Experiment A are thus reported in **Figure 4**. Those pertaining to the carboxylic derivatives of OA (OAox), oleacin (Olea ox) and oleocanthal (Oleo ox) and to the same derivatives for elenolic (EA ox) and decarboxymethyl-elenolic (EDA ox) acids are reported in **Figure 5**. Symbols represent the average value of normalized XIC peak areas, whereas error bars indicate the range of values observed for the two replicated extractions/analyses performed on each EVOO sample. Symbols were linked by lines just to facilitate a comparison of trends found under different conditions. As indicated by error bars reported in **Figures 4** and **5**, a good reproducibility was achieved for extraction and analysis of secoiridoids and related compounds, since the half width of bars

usually corresponded to 5-8% of the related average value, with only occasional higher values (up to 15%) observed. These results confirmed data obtained during our previous studies based on the same extraction protocol[24-26]. Note that the analytical reproducibility, included into the one described so far, was previously assessed in our laboratory by performing four replicated RPLC-ESI-FTMS analyses on the extract obtained from another EVOO, and was found to be 1-2%, according to the considered analyte.

We wish to emphasize that normalization of analyte XIC peak areas to that of the IS oleuropein played a key role in keeping inter-analysis variability at acceptable levels, compensating for instrumental response fluctuations occurring over the long time range of the experiments. This feature, joined to the good extraction reproducibility achieved, enabled the consideration of just two replicates per sample. Such a choice was fundamental to complete the LC-MS analyses of all extracts obtained after a certain storage time as rapidly as possible, thus limiting the delay between analysis and sampling of olive oil from containers. It is also worth noting that we did not attempt a calibration-based quantification of the secoiridoids under evaluation; the first reason for this choice was the lack of reliable standards both for OA and LA and for all the detected oxidized derivatives of secoiridoids. Moreover, due to the potential presence of matrix effects, namely, the competition for ionization between partially co-eluting isoforms of secoiridoids and between them and further eventual co-extracted EVOO components, a reliable calibration would have required the choice of the standard addition method for each sample. However, this procedure would have been incompatible with the need to analyze rapidly several samples after a certain storage time. Nonetheless, normalized XIC peak

areas enabled a reliable evaluation of the time evolution for a certain compound under specific storage conditions.

The starting values (time 0) of normalized responses for OA, LA, oleacin and oleocanthal were in accordance with those previously observed for other Apulian olive oils obtained from *Coratina* olives and using a three-phase horizontal centrifugation[26]. On the other hand, initial normalized responses for oxidized derivatives were almost negligible (see **Figure 5**), thus confirming the efficiency of strategies adopted to protect the oil from oxidation before starting storage experiments. Once storage was started, major secoiridoids underwent a decrease in response (and, consequently, in concentration) under each examined condition (see **Figure 4**). In particular, the outcome obtained for storage in dark glass and under nitrogen (see filled triangles in the figure) was in general accordance with experiments performed during most other studies, all using dark glass for storage, in which specific secoiridoids were monitored for long times (up to 22 months) and without deliberate exposure to oxygen[29,30,35]. Further interesting, and somewhat surprising, results were obtained for the other three setups of Experiment A. Indeed, when the exposure to light was hindered by using a dark glass bottle for storage, the deliberate, periodical introduction of atmospheric oxygen in the bottle headspace (see filled squares in the figure) did not result in a significantly more pronounced degradation, compared to the setup involving headspace saturation with nitrogen. However, this was not the case of storage experiments in which exposure to light was permitted using clear glass bottles; in fact, when the EVOO was exposed both to light and, periodically, to oxygen (see empty squares in **Figure 4**) the degradation was generally more remarkable than when the bottle headspace was saturated with nitrogen (see empty triangles), although comparable final responses for the two setups were found after 6 months for OA and oleacin. Therefore, the synergy of light and oxygen exposure

589 was confirmed as a key factor in prompting the degradation of secoiridoids. On the other hand,
590 the observation of a significant decrease even when the bottle headspace was saturated with
591 nitrogen was partially unexpected. One of the possible interpretations of this outcome could be
592 the contemporary occurrence of hydrolytic degradation, with transformation of major
593 secoiridoids into their constituents, i.e., EA/EDA and tyrosol/3-hydroxytyrosol. However, trends
594 observed for oxidative by-products of OA, oleacin and oleocanthal, shown in **Figure 5**, indicated
595 that this was not the only degradative pathway. In fact, an increase in the incidence of the
596 carboxylic derivatives of the three secoiridoids was clearly observed even when the heaspace of
597 the glass bottles was saturated with nitrogen, although the deliberate introduction of oxygen led
598 to an enhancement in the extent of oxidation. A possible explanation for the observation of an
599 oxidative degradation even when nitrogen is introduced in the bottle headspace could be related
600 to the solubility of oxygen in olive oil. A maximum oxygen concentration of ca. 36 mg/L (ca. 1.1
601 mM) has been estimated for olive oil in equilibrium with air at 1 atm and 25°C[44]. Although oxygen
602 saturation is usually not reached during EVOO production, with a further decrease expected
603 when specific steps of the production process (e.g., malaxation and horizontal/vertical
604 centrifugations) are performed under a nitrogen atmosphere[44], the typical concentrations of
605 dissolved oxygen, close to 10 mg/L, are not negligible. Residual oxygen dissolved in the oil matrix
606 might thus be responsible for oxidation of secoiridoids (at least OA, oleacin and oleocanthal,
607 according to our data), even when the bottle headspace is saturated with nitrogen.

608 The influence of hydrolytic processes on the content of major secoiridoids during storages
609 related to Experiment A was evaluated by monitoring the normalized XIC peak areas of elenolic
610 (EA) and decarboxymethyl- (EDA) elenolic acid, as such or in the oxidized form (EA ox/EDA ox),
611 and of tyrosol and 3-hydroxytyrosol. The lower panels of **Figure 5** report data referred to oxidized

612 EA and EDA, showing a steady increase under any condition, with the expected positive synergy
613 between light and oxygen. Once again, the additional effect of oxygen purposely introduced in
614 the bottle headspace was hardly observed when dark bottles were used. The consequences of
615 hydrolytic degradation can be appreciated by graphs shown in **Figure S8** of the Supporting
616 Information, where trends observed for EA, EDA, 3-hydroxy-tyrosol and tyrosol are reported. The
617 release of EA and EDA upon hydrolysis of the ester bond included in major secoiridoids structures
618 can be easily appreciated, although a stabilization seemed to be reached for EA after 3 months
619 of storage. According to data shown for oxidized forms of EA and EDA in **Figure 5**, this outcome
620 could be due to an enhanced oxidation in the former case, that would transform a more relevant
621 part of the EA released by hydrolytic processes into the corresponding oxidized derivative. In any
622 case, the accumulation of EA and EDA was significantly less relevant for the EVOO exposed to
623 light and oxygen (see empty squares in the corresponding panels of **Figure S8**), due to enhanced
624 oxidation. As far as tyrosol and 3-hydroxytyrosol are concerned, the respective graphs in **Figure**
625 **S8** indicate a comparable increase in almost all conditions, being slightly more pronounced only
626 for the EVOO stored in the clear glass bottle and exposed periodically to atmospheric oxygen.
627 Interestingly, trends observed for the two phenolic compounds in the EVOO stored in a dark glass
628 bottle and without deliberate exposure to oxygen are in accordance, over a 6 months time range,
629 with those reported in previous studies dedicated to storage under similar conditions[27-29, 30]. They
630 clearly confirm the occurrence of hydrolysis on major secoiridoids, although some further
631 transformation of tyrosol and 3-hydroxytyrosol becomes increasingly relevant during storage.
632 According to Brenes *et al.*[28] this transformation likely consists in oxidation of their phenolic OH
633 group(s), with introduction of C=O groups in the molecular structure (for example, a *o*-
634 benzoquinone is expected to be formed in the case of 3-hydroxy-tyrosol). Unfortunately, such

635 modification hinders the subsequent ionization, and, consequently, the MS detection, since the
636 phenolic OH group deprotonation is the most important ionization mechanism occurring for
637 tyrosol and 3-hydroxytyrosol under ESI conditions. For this reason, very low signals, reasonably
638 due to the deprotonation of the alcoholic OH group remaining on the structure of oxidized tyrosol
639 and 3-hydroxytyrosol, were obtained when ion currents were tentatively extracted for these by-
640 products from RPLC-ESI(-)-FTMS data referred to experiment A.

641 Based on the lack of detection of the corresponding carboxylic acid, the progressive
642 degradation of ligstroside aglycone upon storage, inferred from data in **Figure 4**, can be supposed
643 to be mainly hydrolytic, with generation of EA and tyrosol as the main by-products, at least over
644 a 6 months time range. The process could be responsible for the more significant increase
645 observed for EA, compared to that of EDA, under similar storage conditions (see the ordinate
646 scales of the corresponding graphs in **Figure S8**). On the other hand, considering values of
647 normalized XIC peak areas shown in **Figure 5** and supposing negative ionization yields to be
648 similar for secoiridoids oxidized to carboxylic acids (since a COOH group is always the most likely
649 ionization site in this case), oleocanthal appears as the compound more subjected to oxidation
650 during storage. In fact, the normalized peak area of its carboxylic derivative after 6 months of
651 storage was systematically higher than those referred to other oxidized by-products.

652

653 **Evolution of major secoiridoids and of their oxidative/hydrolytic by-products in EVOO during**
654 **prolonged storage in containers manufactured using different materials and with periodic**
655 **exposure to atmospheric oxygen**

656 As discussed before, the eventual influence of the container material and shape on the
657 evolution of major secoiridoids and of their main oxidative and hydrolytic by-products in EVOO

658 stored for long times (up to six months) and periodically exposed to atmospheric oxygen was
659 studied by comparing the results obtained for dark glass, stainless steel, ceramics and PET
660 containers shown in **Figure S1**. Graphs reporting the evolution of normalized XIC peak areas for
661 OA, LA, oleacin and oleocanthal are shown in **Figure 6**. Not unexpectedly, the higher degradation
662 rate was observed for all the four compounds when the clear PET bottle was used for storage,
663 with oleacin and oleocanthal reaching quite low responses after 6 months. The dark glass bottle
664 proved to be the best option, whereas ceramics and stainless steel containers exhibited an
665 intermediate behavior, with an only slightly less pronounced degradation observed for the metal
666 container despite the fact that the headspace available in the ceramics jar was almost double as
667 large as the one estimated for the stainless steel can (see values reported in **Figure S1**). It is worth
668 noting that the limited headspace available in the case of the glass bottle (ca. 10% of the initial
669 oil volume) could have played a role in reducing the degradative damage, at least the one related
670 to oxidation processes. Another interesting feature easily inferred from graphs in **Figure 6** was
671 the similarity of trends observed for the two secoiridoids embedding 3-hydroxytyrosol in their
672 structure (OA and oleacin), on one side, and for the two including tyrosol (LA and oleocanthal).
673 Indeed, a more evident decrease was observed for the former two compounds up to three
674 months, then the degradation rate seemed to be reduced significantly in the subsequent three
675 months. In tyrosol-including secoiridoids the decrease was more regular over the entire time
676 range of the experiment. Regardless of the container adopted, LA confirmed to be the secoiridoid
677 less susceptible to degradation over time, with the lowest percentual decrease observed after 6

678 months. The already described resistance to oxidation to COOH of the C=O group(s) of LA
679 isoforms could be primarily responsible for this outcome.

680 Further insights into the observed evolution of precursors could be obtained by
681 monitoring carboxylic derivatives of OA, oleacin, oleocanthal, EA and EDA, whose normalized XIC
682 peak areas are shown in graphs reported in **Figure 7**. Clear PET was still confirmed as the worst
683 material for EVOO storage, with values for all the five derivatives being systematically higher,
684 even remarkably (see the graph referred to the carboxylic derivative of oleocanthal, *alias* Oleo
685 ox), after 2 or 3 months of storage, according to the compound. In this case the stainless steel
686 can showed a very good performance, keeping all the compounds at the lowest levels after long
687 storage times. From the point of view of oxidized derivatives, ceramics and dark glass generally
688 showed a similar behavior, intermediate between PET and stainless steel. Also in this case, like
689 for Experiment A, the monitoring of hydrolytic derivatives of the EVOO four major secoiridoids
690 was useful to provide a comprehensive interpretation of data. Graphs reported in **Figure S9** of
691 the Supporting Information describe the time evolution of EA, EDA, 3-hydroxytyrosol and tyrosol.
692 The general feature observed was the sigmoidal-like shape of trends, suggesting the occurrence
693 of further transformation of those by-products after long storage times. If PET-related data are
694 considered, the limitation of EA and EDA accumulation after 3-6 months could be due to the
695 remarkable increase of the corresponding oxidized forms (see **Figure 7**), thus suggesting the
696 contribution of oxidation processes occurring on both compounds after their release upon
697 hydrolysis of the ester bond of the original secoiridoids. The concentration of oxidized forms of
698 EA and EDA could be increased also by the contribution due to the hydrolysis occurring on the
699 previously formed carboxylic derivatives of OA and oleacin, for EA, and of oleocanthal, for EDA.
700 The overall scenario observed for PET was as expected, with the synergy between continuous

exposure to light and enhanced oxygen availability, due to permeation of the gas through the container walls, resulting in a remarkable incidence of oxidative degradation.

Data interpretation was more complex for the other three packaging materials. The largest accumulation of hydrolytic by-products was observed in the case of stainless steel (see **Figure S9**). This outcome could be related to the lower incidence of their transformation into the corresponding oxidized products, consistent with the lowest incidence observed also for carboxylic derivatives of major secoiridoids (see **Figure 7**). The data suggest that the stainless-steel container was the best in terms of protection of stored EVOO from the additional exposure to oxygen resulting from the periodical opening of the container. We suppose that the specific conformation of the anti-refill device embedded into the neck of the stainless-steel container could have played a relevant role in determining this effect, simply by physically limitating the renewal with air of the container headspace. It is worth mentioning that the more significant accumulation of 3-hydroxytyrosol and tyrosol inferred from graphs in **Figure S9** indicates hydrolysis as a relevant pathway for the degradation of the EVOO original secoiridoids in the stainless steel container, whereas a less pronounced hydrolysis occurred in the case of dark glass. The following general indication thus emerged after comparing data shown in **Figures 6**, **7** and **S9**: the dark glass bottle enabled a better protection of secoiridoids from hydrolytic degradation, whereas stainless steel ensured, likely due to the peculiar construction of the container, a more limited access of air, and hence of oxygen, when the container was opened periodically, thus contributing to keep the oxidative degradation of secoiridoids at the lowest levels, despite the higher volume of the headspace (see **Figure S1**). The overall effect was a slightly lower degradation rate in the case of dark glass bottle (see **Figure 6**). As for ceramics, the protection from oxidative degradation was generally not as good as that offered by dark glass or stainless-

steel (see data in **Figure 7**); the effect of the large available headspace (see **Figure S1**) likely played a role from this point of view, thus a careful choice of the ratio between oil volume and container capacity should be considered by producers using ceramics jars for EVOO commercialization, at least if the protection of secoiridoids from oxidative degradation during the subsequent domestic use of the container is a concern.

A final consideration can be made about the possible effects that the accumulation of oxidized derivatives described in the present paper may have on the health benefits related to olive oil consumption. A recent study focused on oleocanthalic acid has evidenced that this derivative might have neuroprotective activity, with benefits for patients affected by pathologies like Alzheimer's disease[37]. On the other hand, the oxidation to a COOH group of one of the C=O groups included in open forms of olive oil secoiridoids might impair their behavior as glutaraldehyde-like structures, which has been reported as a key for the protein denaturing/cross linking effects played by those isoforms in olive plants, in which they can act as defensive molecules[45]. Further studies will be required to verify if the partial loss of this feature induced by oxidation of di-aldehydic secoiridoids in stored olive oil might have relevance on the benefits of the product for human health.

Conclusions

The RPLC-ESI-FTMS-based careful monitoring of major secoiridoids and of their more relevant oxidative/hydrolytic by-products enabled a detailed study of the effects on these compounds of EVOO storage for up to 6 months under different conditions, including exposure to light and/or atmospheric oxygen and container shape and material. Carboxylic derivatives of oleuropein aglycone, oleacin and oleocanthal were found as relevant oxidative by-products of secoiridoids in stored EVOO samples. A comparative experiment involving clear or dark glass bottles typically

749 adopted for olive oil commercialization and the eventual resaturation of headspace with
750 nitrogen, showed that oxygen dissolved into oil played a not negligible role in secoiridoid
751 oxidation to carboxylic acids. In any case, the extent of this oxidative degradation was more
752 remarkable when exposure to light was also permitted, using a clear glass bottle for storage. In
753 a parallel development of the study, the comparison of storage effects was made using three
754 typical commercial containers for olive oil, made of dark glass, ceramics and stainless-steel
755 respectively, that were periodically exposed to atmospheric oxygen to simulate a domestic use.
756 As a negative control, a clear PET bottle was also adopted in the experiment. Likely due to the
757 peculiar presence of an anti-refill device in the neck, hindering the re-introduction of oxygen
758 during each opening, the stainless steel container offered the best protection against secoiridoid
759 oxidation to carboxylic derivatives, followed by the dark glass bottle. On the other hand, the
760 more limited extent of hydrolytic degradation, likely due to the lower extension of the
761 headspace/oil interface, made the dark glass bottle the best container if the focus was on the
762 integrity of original secoiridoids. Data obtained during the present study show that the complex
763 degradative phenomena occurring on EVOO secoiridoids during storage can be monitored in
764 detail by liquid chromatography-high resolution/accuracy mass spectrometry. The potential of
765 this approach opens very interesting perspectives in terms of control of the integrity of
766 secoiridoids during storage of EVOO under any possible condition.

767

768

769 **ACKNOWLEDGMENTS**

770 This work was supported by the following projects: PONa3_00395/1 “BIOSCIENZE & SALUTE
771 (B&H)”, funded by the Italian *Ministero per l'Istruzione, l'Università e la Ricerca* (MIUR) and AGER
772 2016-0169 “VIOLIN”, funded by *Fondazioni in Rete per la Ricerca Agroalimentare* (AGER).

773

774 ## Conflict of interest

775

776 The Authors have no conflict of interest to declare.

777

778 ## Supporting Information

779

780 Photographs and dimensions of containers adopted for EVOO storage experiments (Figure S1);
781 schematic representation of EVOO storage experiments (Figure S2); fragmentation pathways
782 hypothesized to identify *Open Forms II* of oleacin and oleocanthal and *Closed Forms I* of
783 oleocanthal (Figure S3); fragmentation pathways hypothesized to identify *Closed Forms I* of
784 oleocanthal oxidized to carboxylic acid (Figure S4); fragmentation pathways hypothesized to
785 identify *Open Forms II* of oleacin and oleocanthal oxidized to carboxylic acid (Figure S5); key
786 product ions considered to identify open- or closed-structure isoforms of oleuropein aglycone
787 oxidized to carboxylic acid (Figure S6); comparison between eXtracted Ion Current (XIC)
788 chromatograms referred to hydrolytic by-products of EVOO secoiridoids, obtained after 6-
789 months storage in a dark glass bottle periodically exposed to atmospheric oxygen (Figure S7);
790 comparisons between time evolution of XIC peak areas obtained for hydrolytic by-products of
791 secoiridoids in EVOO stored up to six months in dark/clear glass bottles with/without periodical
792 exposure to atmospheric oxygen (Figure S8); comparisons between time evolution of XIC peak
793 areas obtained for hydrolytic by-products of secoiridoids in EVOO stored up to six months in four
794 different types of containers (see Figure S1) with periodical exposure to atmospheric oxygen
795 (Figure S9).

796

797

References

1. ABoskou, D. *Olive and Olive Oil Bioactive Constituents*, AOCS Press: Urbana, IL, 2015.

2. Owen, R.W.; Mier, W.; Giacosa, A.; Hull, W.E.; Spiegelhalder, B.; Bartsch, H. Phenolic compounds and squalene in olive oils: the concentration and antioxidant potential of total phenols, simple phenols, secoiridoids, lignans and squalene. *Food Chem. Toxicol.* **2000**, *38*, 647-659.

3. Servili, M.; Montedoro, G.F. Contribution of phenolic compounds to virgin olive oil quality. *Eur. J. Lip. Sc. Tech.* **2002**, *104*, 602-613.

4. Andrews, P.; Busch, J.; de Joode, T.; Groenewegen, A.; Alexandre H. Sensory properties of virgin olive oil polyphenols: identification of deacetoxy-ligstroside aglycon as a key contributor to pungency. *J. Agric. Food Chem.* **2003**, *51*, 1415–1420.

5. Beauchamp, G.K.; Keast, R.S.; Morel, D.; Lin, J.; Pika, J.; Han, Q.; Lee, C.H.; Smith, A.B.; Breslin, P.A. Phytochemistry: ibuprofen-like activity in extra-virgin olive oil. *Nature* **2005**, *437*, 45-46.

6. Tripoli, E.; Giammanco, M.; Tabacchi, G.; Di Majo, D.; Giammanco, S.; La Guardia, M. The phenolic compounds of olive oil: structure, biological activity and beneficial effects on human health. *Nutr. Res. Rev.* **2005**, 18, 98-112.

7. Bendini, A.; Cerretani, L.; Carrasco-Pancorbo, A.; Gomez-Caravaca, A.M.; Segura-Carretero, A.; Fernandez-Gutierrez, A.; Lercker, G. Phenolic Molecules in Virgin Olive Oils: a Survey of Their Sensory Properties, Health Effects, Antioxidant Activity and Analytical Methods. An Overview of the Last Decade. *Molecules*. **2007**, *12*, 1679-1719.

8. Cicerale, S.; Breslin, P.A.S.; Beauchamp, G.K.; Keast, R.S.J. Sensory characterization of the irritant properties of oleocanthal, a natural anti-inflammatory agent in extra virgin olive oils. *Chem. Sens.* **2009**, *34*, 333-339.

9. Hassen, I.; Casabianca, H.; Hosni, K. Biological activities of the natural antioxidant oleuropein: exceeding the expectation – A mini-review. *J. Func. Foods.* **2015**, *18*, 926-940

10. Gariboldi, P.; Jommi, G.; Verotta, L. Secoiridoids from Olea Europaea. *Phytochem.* **1986**, *25*, 865-869.

11. Montedoro, G.F.; Servili, M.; Baldioli, M.; Selvaggini, R.; Miniati, E.; Macchioni, A. Simple and hydrolyzable compounds in virgin olive oil. 3. Spectroscopic characterizations of the secoiridoid derivatives. *J. Agric. Food Chem.* **1993**, *41*, 2228-2234.

12. Limiroli, R.; Consonni, R.; Ottolina, G.; Marsilio, V.; Bianchi, G.; Zetta, L. 1 H and 13 C NMR characterization of new oleuropein aglycones. *J. Chem. Soc., Perkin Trans. 1.* **1995**, *12*, 1519-1523.

13. De Nino, A.; Mazzotti, F.; Perri, E.; Procopio, A.; Raffaelli, A.; Sindona, G. Virtual freezing of the hemiacetal–aldehyde equilibrium of the aglycones of oleuropein and ligstroside present in olive oils from Carolea and Coratina cultivars by ionspray ionization tandem mass spectrometry. *J. Mass Spectrom.* **2000**, *35*, 461-467.

14. Impellizzeri, J.; Lin, J. Simple High-Performance Liquid Chromatography Method for the Determination of Throat-Burning Oleocanthal with Probated Anti-inflammatory Activity in Extra Virgin Olive Oils. *J. Agric. Food Chem.* **2006**, *54*, 3204-3208.

15. Fu, S.; Arraez-Roman, D.; Menendez, J.A.; Segura-Carretero, A.; Fernandez-Gutierrez, A. Characterization of isomers of oleuropein aglycon in olive oils by rapid-resolution liquid chromatography coupled to electrospray time-of-flight and ion trap tandem mass spectrometry. *Rapid Comm. Mass Spectr.* **2009**, *23*, 51-59.

16. Perez-Trujillo, M.; Gomez-Caravaca, A.M.; Segura-Carretero, A.; Fernandez-Gutierrez, A.; Parella, T. Separation and Identification of Phenolic Compounds of Extra Virgin Olive Oil from Olea europaea L. by HPLC-DAD-SPE-NMR/MS. Identification of a New Diastereoisomer of the Aldehydic Form of Oleuropein Aglycone. *J. Agric. Food Chem.* **2010**, 58, 9129–9136.

17. Kanakis, P.; Termentzi, A.; Michel, T.; Gikas, E.; Halabalaki, M.; Skaltsounis, A.-L. From Olive Drupes to Olive Oil. An HPLC-Orbitrap-based Qualitative and Quantitative Exploration of Olive Key Metabolites. *Planta Med.* **2013**, *79*, 1576-1587.

18. Vichi, S.; Cortés-Francisco, N.; Caixach, J. Insight into virgin olive oil secoiridoids characterization by high-resolution mass spectrometry and accurate mass measurements. *J. Chromat. A.* **2013**, *1301*, 48-59.

19. Karkoula, E.; Skantzari, A.; Melliou, E.; Magiatis, P. Quantitative Measurement of Major Secoiridoid Derivatives in Olive Oil Using qNMR. Proof of the Artificial Formation of Aldehydic Oleuropein and Ligstroside Aglycon Isomers. *J. Agric. Food Chem.* **2014**, *62*, 600-607.

20. Diamantakos, P.; Velkou, A.; Killday, K.B.; Gimisis, T.; Melliou, E.; Magiatis, P. Oleokoronal and oleomissional: new major phenolic ingredients of extra virgin olive oil. *Olivae*. **2015**, *122*, 22-33

21. Adhami, H.; Zehl, M.; Dangl, C.; Dorfmeister, D.; Stadler, M.; Urban, E.; Hewitson, P.; Ignatova, S.; Krenn, L. Preparative isolation of oleocanthal, tyrosol, and hydroxytyrosol from olive oil by HPCCC. *Food Chem.* **2015**, *170*, 154-159.

22. Sanchez de Medina, V.; Miho, H.; Melliou, E.; Magiatis, P.; Priego-Capote, F.; Luque de Castro, M.D. Quantitative method for determination of oleocanthal and oleacein in virgin olive oils by liquid chromatography–tandem mass spectrometry. *Talanta.* **2017**, *162*, 24-31.

23. Celano, R.; Piccinelli, A.L.; Pugliese, A.; Carabetta, S.; di Sanzo, R.; Rastrelli, L.; Russo, M. Insights into the Analysis of Phenolic Secoiridoids in Extra Virgin Olive Oil. *J. Agric. Food*

Chem. **2018**, *66*, 6053-6063.

24. Abbattista, R.; Losito, I.; De Ceglie, C.; Castellaneta, A.; Calvano, C.D.; Palmisano, F.; Cataldi, T.R.I. A comprehensive study of oleuropein aglycone isomers in olive oil by enzymatic/chemical processes and liquid chromatography-Fourier transform mass spectrometry integrated by H/D exchange. *Talanta*. **2019**, *205*, 120107.

25. Abbattista, R.; Losito, I.; De Ceglie, C.; Basile, G.; Calvano, C.D.; Palmisano, F.; Cataldi, T.R.I. Structural characterization of the ligstroside aglycone isoforms in virgin olive oils by liquid chromatography–high-resolution Fourier-transform mass spectrometry and H/D exchange. *J. Mass Spectrom.* **2019**, *54*, 843–855.

26. De Ceglie, C.; Abbattista, R; Losito, I.; Castellaneta, A.; Calvano, C.D.; Bianco, G.; Palmisano, F.; Cataldi, T.R.I. Influence of Horizontal Centrifugation Processes on the Content of Phenolic Secoiridoids and Their Oxidized Derivatives in Commercial Olive Oils: An Insight by Liquid Chromatography−High-Resolution Mass Spectrometry and Chemometrics. *J. Agric. Food Chem.* **2020**, *68*, 3171–3183.

27. Cinquanta, L.; Esti, M.; La Notte, E. Evolution of Phenolic Compounds in Virgin Olive Oil During Storage. *J. Am. Oil Chem. Soc.* **1997**, *74*, 1259-1263.

28. Brenes, M.; Garcia, A.; Garcia, P.; Garrido, A. Acid Hydrolysis of Secoiridoid Aglycons during Storage of Virgin Olive Oil. *J. Agric. Food Chem.* **2001**, *49*, 5609 - 5614.

29. Morello, J.R.; Motilva, M.J.; Tovar, M.J.; Romero, M.P. Changes in commercial virgin olive oil (cv Arbequina) during storage, with special emphasis on the phenolic fraction. *Food Chem*. **2004**, *85*, 357-364.

30. Sicari, V.; Giuffrè, A.M.; Louadj, L.; Poiana, M. Evolution of phenolic compounds of virgin olive oil during 12 months storage. *Rivista Italiana delle Sostanze Grasse* **2010**, *87*, 109-116.

31. Lozano-Sánchez, J.; Bendini, A.; Quirantes-Piné, R.; Cerretani, L.; Segura-Carretero, A.; Fernández-Gutiérrez, A. Monitoring the bioactive compounds status of extra-virgin olive oil and storage by-products over the shelf life. *Food Contr.* **2013**, *30*, 606-615.

32. Krichene, D.; Desamparados Salvador, M., Fregapane, G.; Stability of Virgin Olive Oil Phenolic Compounds during Long-Term Storage (18 Months) at Temperatures of 5-50°C. *J. Agric. Food Chem.* **2015**, *63*, 6779-6786.

33. Kotsiou, K., Tasioula-Margari, M. Monitoring the phenolic compounds of Greek extra-virgin olive oils during storage. *Food Chem.* **2016**, *200*, 255-262.

34. Di Stefano, V.; Melilli, M.G. Effect of storage on quality parameters and phenolic content of Italian extra-virgin olive oils. *Nat. Prod. Res.* **2020**, *34*, 78-86.

35. Esposto, S.; Selvaggini, R.; Taticchi, A.; Veneziani, G.; Sordini, B.; Servili, M. Quality evolution

of extra-virgin olive oils according to their chemical composition during 22 months of storage under dark conditions. *Food Chem.* **2020**, *311*, 126044.

36. Angelis, A.; Antoniadi, L.; Stathopoulos, P.; Halabalaki, M., Skaltsounis, L.A. Oleocanthalic and Oleaceinic acids: New compounds from Extra Virgin Olive Oil (EVOO). *Phytochem. Lett.* **2018**, *26*, 190-194.

37. Tsolakou, A.; Diamantakos, P.; Kalaboki, I.; Mena-Bravo, A.; Priego-Capote, F.; Abdallah, I.M; Kaddoumi, A.; Melliou, E.; Magiatis, P. Oleocanthalic Acid, a Chemical Marker of Olive Oil Aging and Exposure to a High Storage Temperature with Potential Neuroprotective Activity. *J. Agric. Food Chem.* **2018**, *66*, 7337-7346.

38. Morales, M.T.; Przybylsky, R. Olive Oil Oxidation. In *Handbook of Olive Oil: Analysis and Properties*; Aparicio-Ruiz, R.; Harwood, J., Eds.; Springer: New York, NY, 2013, pp. 479-522.

39. Hajimohammadi, M.; Safari, N.; Mofakham, H.; Shaabani, A. A new and efficient aerobic oxidation of aldehydes to carboxylic acids with singlet oxygen in the presence of porphyrin sensitizers and visible light, *Tetrahedron Lett.* **2010**, *51*, 4061-4065.

40. Kontominas, M.G. Olive oil packaging: recent developments. In *Olives and Olive Oil as Functional Foods: Bioactivity, Chemistry and Processing*; Kiritsakis, A.; Shahidi, F., Eds.; Wiley, Chichester, UK, 2017, pp. 279-294.

41. Ricciutelli, M.; Marconi, S.; Boarelli, M.C.; Caprioli, G.; Sagratini, G.; Ballini, R.; Fiorini, D. Olive oil polyphenols: A quantitative method by high performance liquid-chromatography-diode-array detection for their determination and the assessment of the related health claim. *J. Chromatogr. A* **2017**, *1481*, 53-63.

42. Carrasco-Pancorbo, A.; Cerretani, L.; Bendini, A.; Segura-Carretero, A.; Lercker, G., Fernandez-Gutierrez, A.; Evaluation of the Influence of Thermal Oxidation on the Phenolic Composition and on the Antioxidant Activity of Extra-Virgin Olive Oils. *J. Agric. Food Chem.* **2007**, *55*, 4771-4780.

43. Bendini, A.; Cerretani, L.; Vecchi, S.; Carrasco-Pancorbo, A; Lercker, G., Protective Effects of Extra Virgin Olive Oil Phenolics on Oxidative Stability in the Presence or Absence of Copper Ions. *J. Agric. Food Chem.* **2006**, *54*, 4880-4887.

44. Parenti, A.; Spugnoli, P.; Masella, P.; Calamai, L. Influence of the extraction process on dissolved oxygen in olive oil, *Eur. J. Lip. Sc. Tech.* **2007**, *109*, 1180-1185.

45. Koudounas, K.; Thomopoulou, M., Michaelidis, C.; Zevgiti E.; Papakostas, G.; Tserou, P.; Daras, G.; Hatzopoulos, P. The C-Domain of Oleuropein β-Glucosidase Assists in Protein Folding and Sequesters the Enzyme in Nucleus, *Plant Phys.*, 2017, 174, 1371-1383.

980
981
982
983
984
985

Figures captions

Figure 1. Molecular structures previously inferred in our laboratory, using RPLC-ESI-FTMS and MS/MS, for the isomeric forms of Oleuropein (OA) and Ligstroside (LA) aglycones and for oleacin and oleocanthal in olive oil [see Refs. 24-26]. The secoiridoid moiety of each structure is emphasized; the nomenclature already used in Refs. 24-26 for isoforms is reported. Chiral (C^5) and stereogenic centres are indicated with an asterisk; wavy bonds evidence the presence of geometrical or configurational isomerism, according to the case.

Figure 2. Comparison between eXtracted Ion Current (XIC) chromatograms obtained for the first isotopologues of $[M-H]^-$ ions of oleuropein aglycone (OA), ligstroside aglycone (LA), oleacin and oleocanthal after the RPLC-ESI-(-)-FTMS analysis of one of the two extracts obtained from the EVOO adopted in the present study before starting with storage experiments (time 0). The XIC trace referred to oleuropein, (internal standard, 100 mg/L concentration), is also shown. See text for details about peaks with underlined retention times.

Figure 3. Comparison between eXtracted Ion Current (XIC) chromatograms obtained for the first isotopologues of $[M-H]^-$ ions of the major secoiridoids, of oleuropein internal standard (100 mg/L) and of the carboxylic derivatives of oleuropein aglycone, oleacin, and elenolic and decarboxymethyl-elenolic acids after the RPLC-ESI-(-)-FTMS analysis of the extract obtained from the EVOO adopted in the present study after 6 months of storage in a dark glass bottle periodically exposed to atmospheric oxygen. OF and CF labels refer, respectively, to *Open Forms II* and *Closed Forms I* isoforms. See text for details about peaks with underlined retention times.

1010 **Figure 4**. Time evolution of XIC peak areas obtained after the RPLC-ESI(-)FTMS analyses of EVOO
1011 extracts by integration of peaks referred to oleuropein and ligstroside aglycones (OA, LA) and to
1012 oleacin and oleocanthal during storage in: i) a dark glass bottle, with (filled squares) or without
1013 (filled triangles) periodical exposure to atmospheric oxygen; ii) a clear glass bottle, with (empty
1014 squares) or without (empty triangles) periodical exposure to atmospheric oxygen. All areas were
1015 normalized to that of oleuropein (100 mg/L) added to the extracts as internal standard. Error
1016 bars represent ranges of values obtained from two replicates performed for each sample.
1017
1018 **Figure 5**. Time evolution of XIC peak areas obtained after the RPLC-ESI(-)FTMS analyses of EVOO
1019 extracts by integration of peaks referred to the carboxylic derivatives of oleuropein (OA ox),
1020 oleacin (Olea ox), oleocanthal (Oleo ox), elenolic acid (EA ox) and decarboxymethyl-elenolic acid
1021 (EDA ox) during storage in: i) a dark glass bottle, with (filled squares) or without (filled triangles)
1022 periodical exposure to atmospheric oxygen; ii) a clear glass bottle, with (empty squares) or
1023 without (empty triangles) periodical exposure to atmospheric oxygen. All areas were normalized
1024 to that of oleuropein (100 mg/L) added to the extracts as internal standard. Error bars represent
1025 ranges of values obtained from two replicates performed for each sample.
1026
1027 **Figure 6**. Time evolution of XIC peak areas obtained after the RPLC-ESI(-)FTMS analyses of EVOO
1028 extracts by integration of peaks referred to oleuropein and ligstroside aglycones (OA, LA) and to
1029 oleacin and oleocanthal during storage in: i) a dark glass bottle (filled squares), ii) a ceramics jar
1030 (filled triangles), iii) a stainless steel can (filled circles), iv) a PET bottle (empty squares),
1031 periodically exposed to atmospheric oxygen (see Figure S1). All areas were normalized to that of
1032 oleuropein (100 mg/L) added to the extracts as internal standard. Error bars represent ranges of

values obtained from two replicates performed for each sample.

Figure 7. Time evolution of XIC peak areas obtained after the RPLC-ESI(-)FTMS analyses of EVOO extracts by integration of peaks referred to the carboxylic derivatives of oleuropein (OA ox), oleacin (Olea ox), oleocanthal (Oleo ox), elenolic acid (EA ox) and decarboxymethyl-elenolic acid (EDA ox) during storage in: i) a dark glass bottle (filled squares), ii) a ceramics jar (filled triangles), iii) a stainless steel can (filled circles), iv) a PET bottle (empty squares), periodically exposed to atmospheric oxygen (see Figure S1). All areas were normalized to that of oleuropein (100 mg/L) added to the extracts as internal standard. Error bars represent ranges of values obtained from two replicates performed for each sample.

Oleuropein Aglycone, OA (R' = OH)
Ligstroside Aglycone, LA (R' = H)

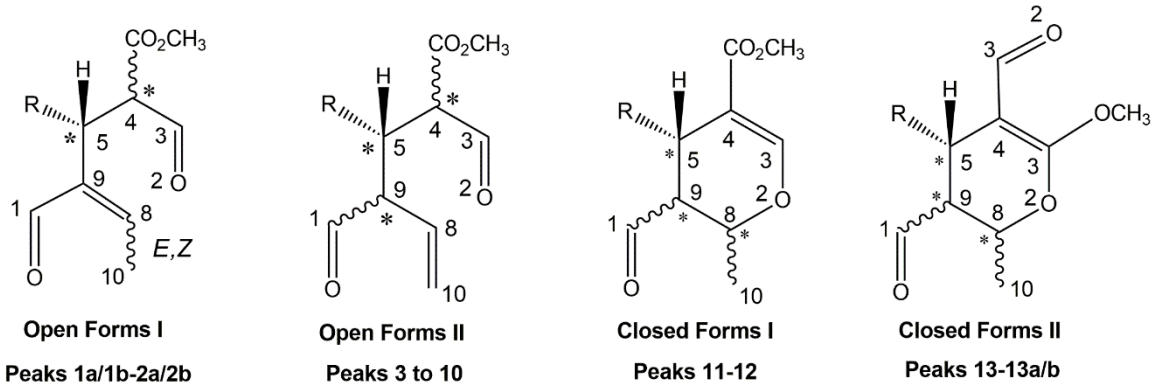

Open Forms I
Peaks 1a/1b-2a/2b

Open Forms II
Peaks 3 to 10

Closed Forms I
Peaks 11-12

Closed Forms II
Peaks 13-13a/b

Oleacin (R' = OH)
Oleocanthal (R' = H)

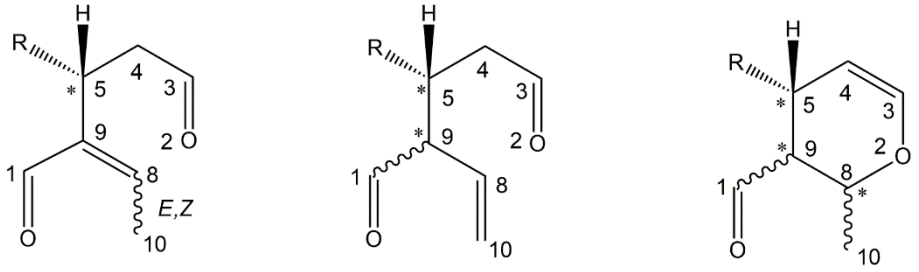

Open Forms I

Open Forms II

Closed Forms I

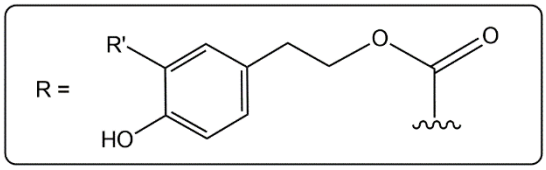

1044

Figure 1.

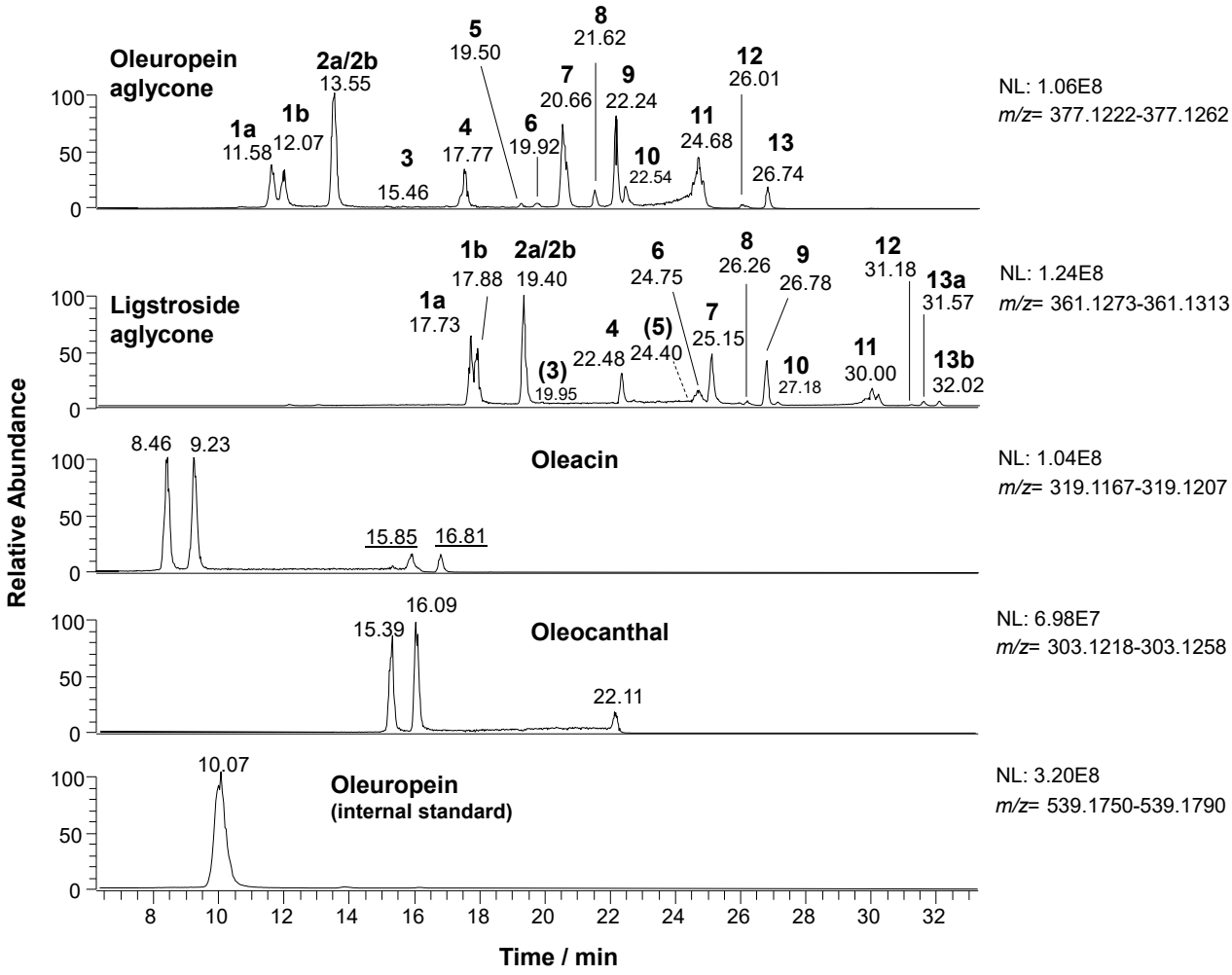

1045

Figure 2.

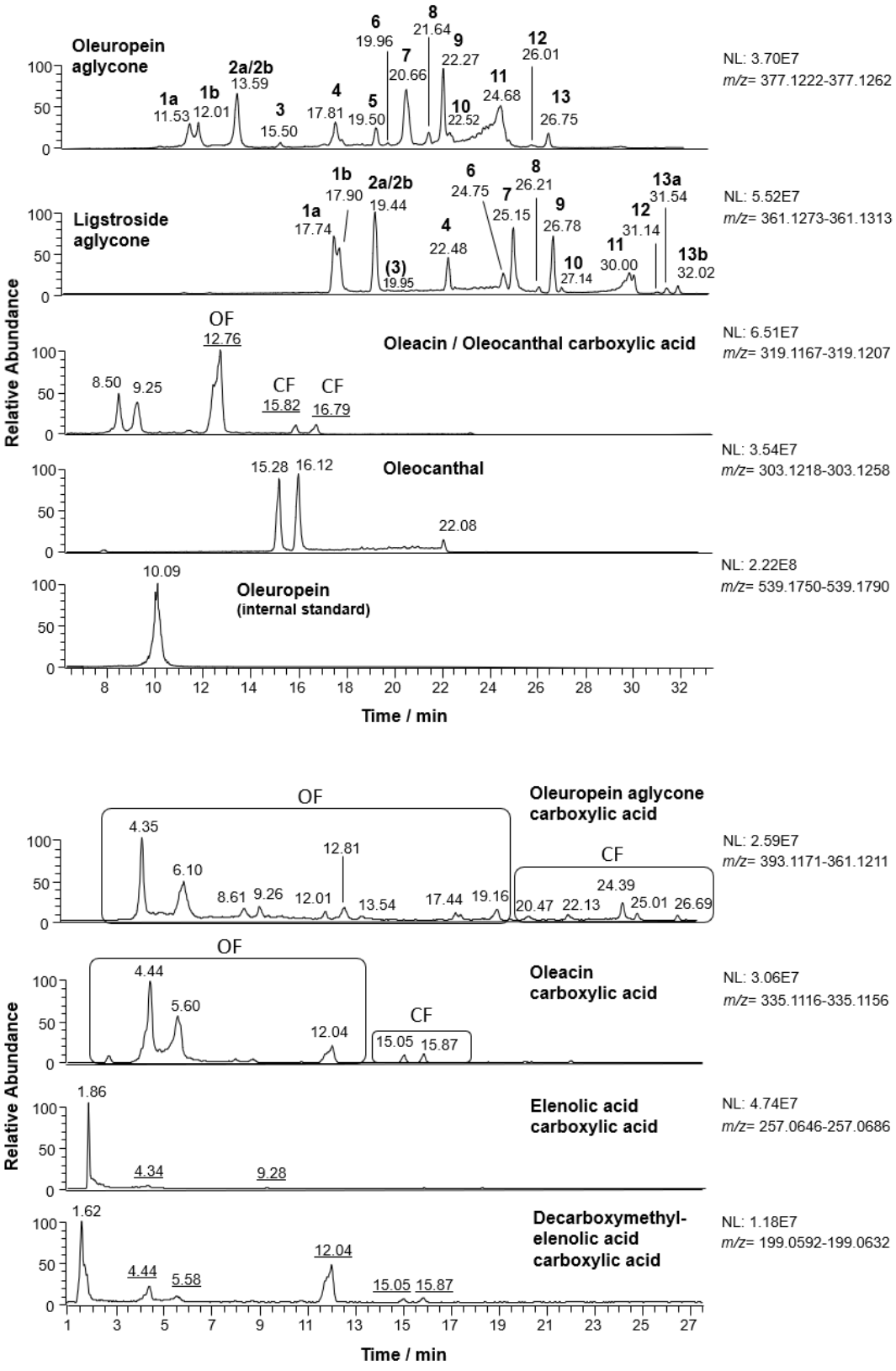

1046

Figure 3.

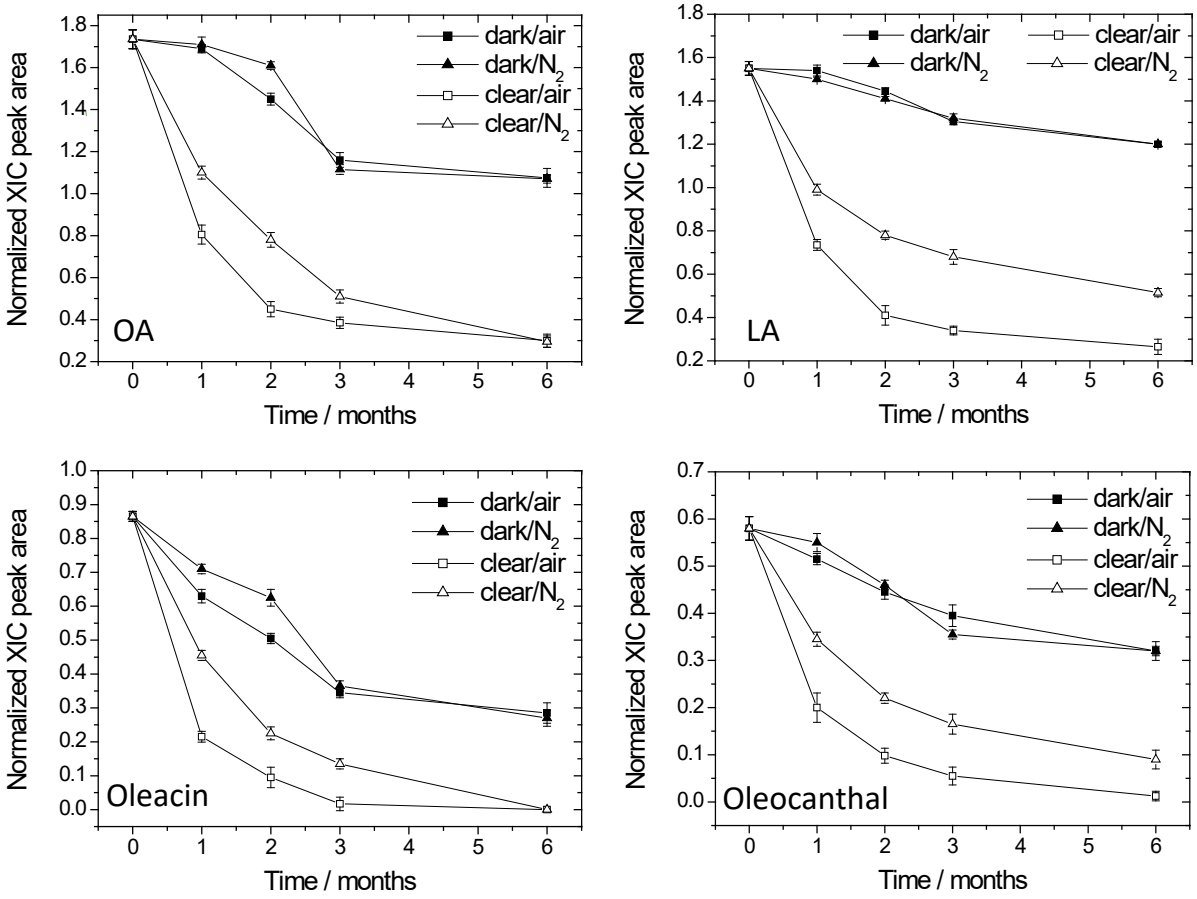

Figure 4.

1047

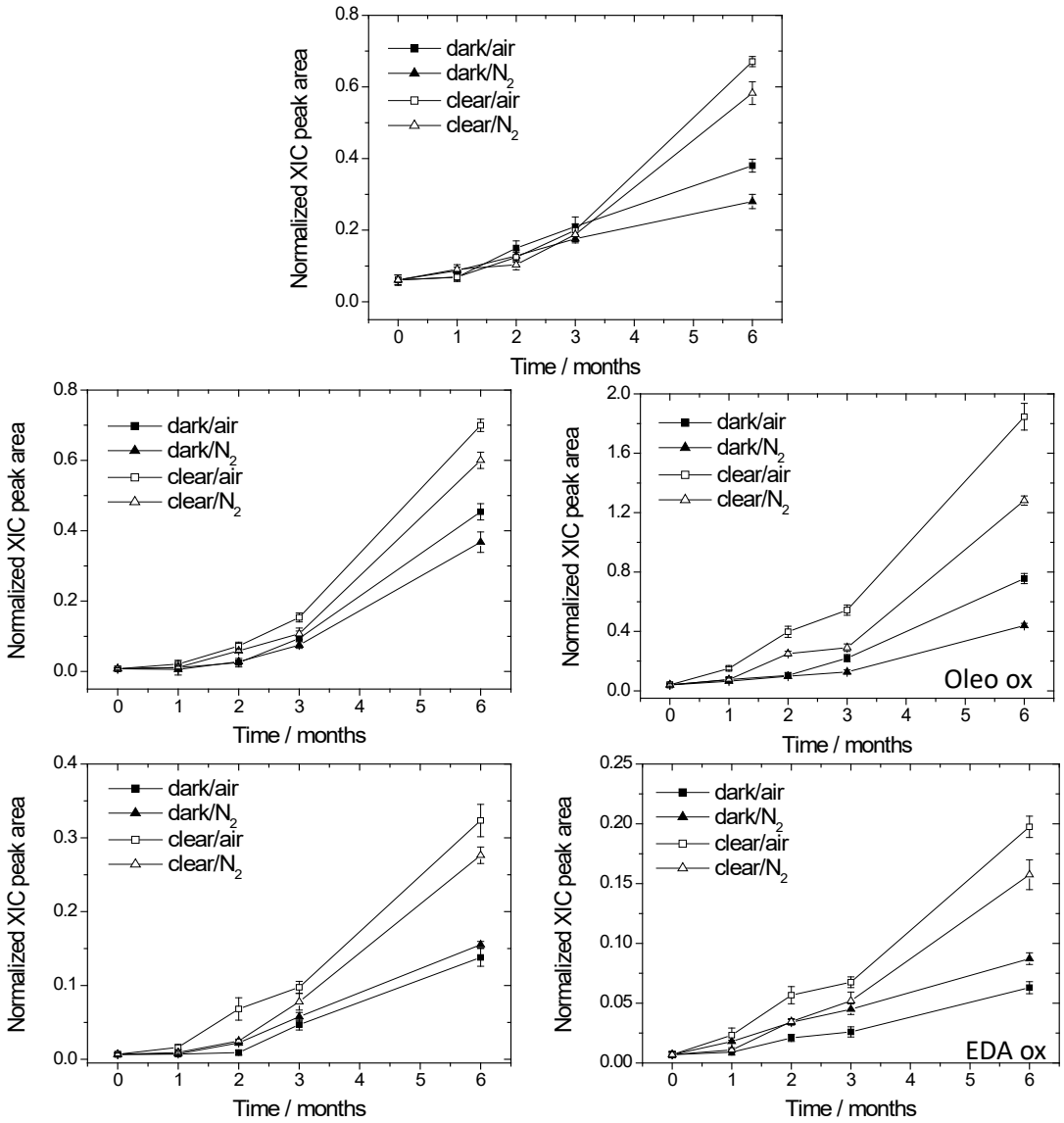

1048

Figure 5.

1049

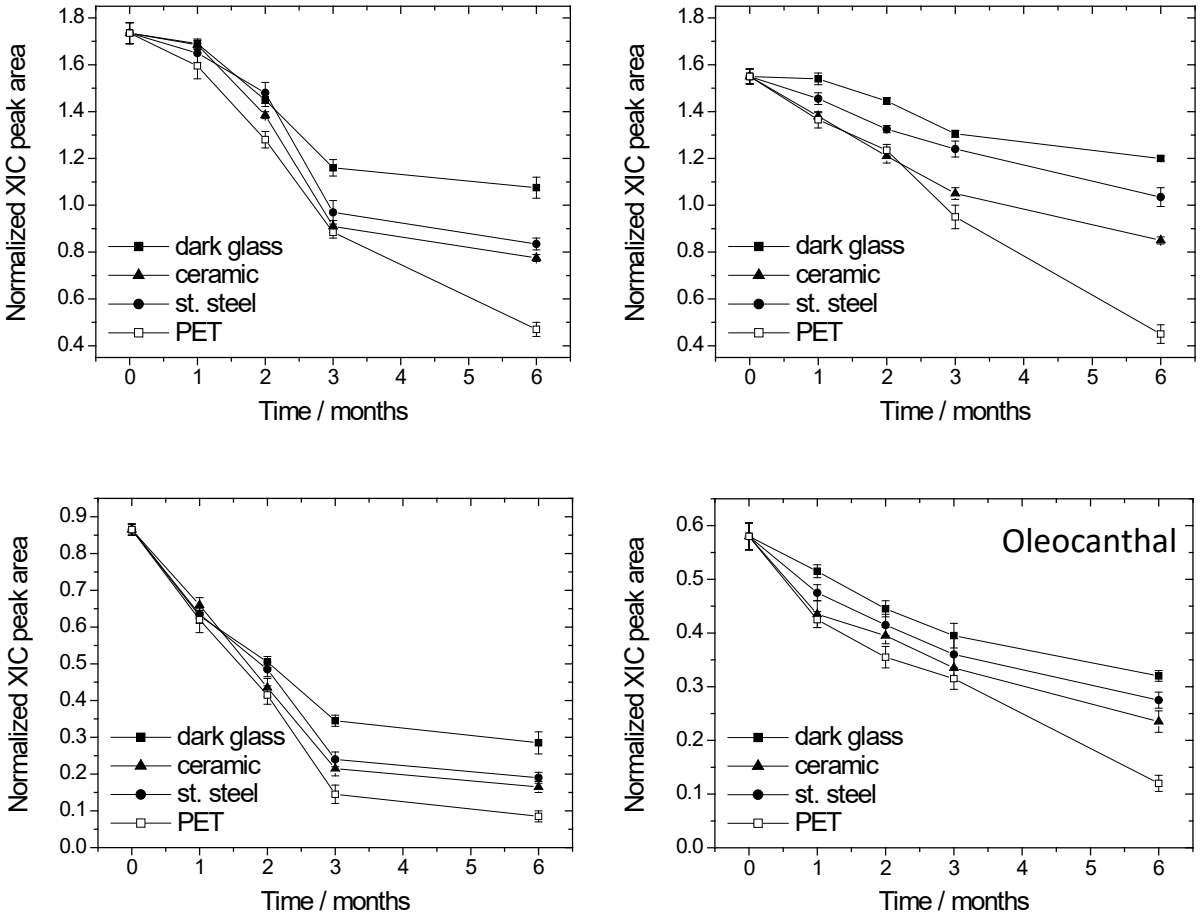

1050

Figure 6.

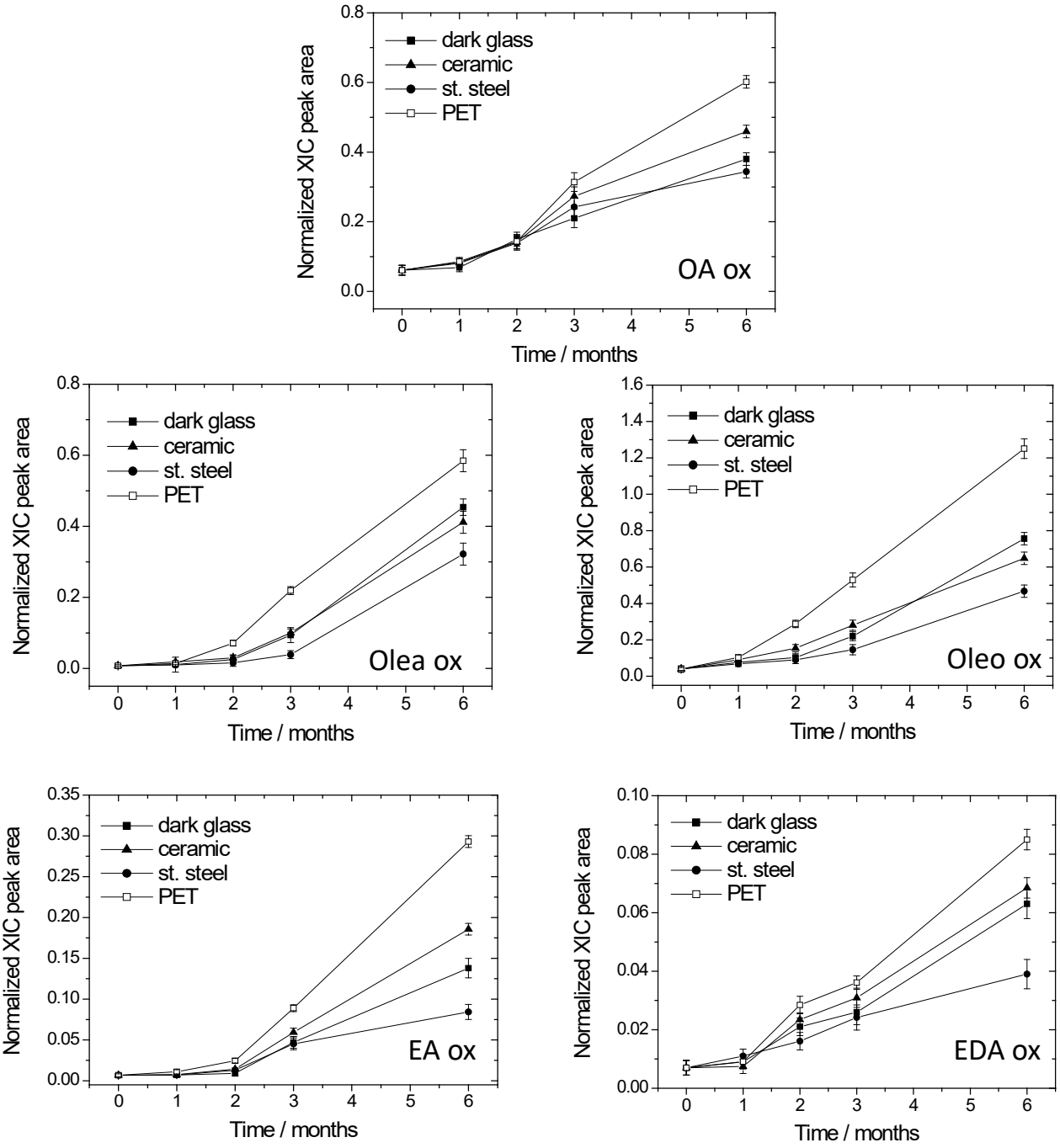
Normalized XIC peak area
Time / months
dark glass
ceramic
st. steel
PET
OA ox
Olea ox
Oleo ox
EA ox
EDA ox

Figure 7.

1053

For Table of Contents Only

1054

1055